Regular Article

blood

HEMATOPOIESIS AND STEM CELLS

Fibrinolytic crosstalk with endothelial cells expands murine mesenchymal stromal cells

Douaa Dhahri,[1] Kaori Sato-Kusubata,[1] Makiko Ohki-Koizumi,[1] Chiemi Nishida,[1,2] Yoshihiko Tashiro,[2] Shinya Munakata,[2] Hiroshi Shimazu,[2] Yousef Salama,[1] Salita Eiamboonsert,[1] Hiromitsu Nakauchi,[3] Koichi Hattori,[1-4,*] and Beate Heissig[1,3,4,*]

[1]Division of Stem Cell Dynamics, [2]Division of Stem Cell Regulation, and [3]Center for Stem Cell Biology and Regenerative Medicine, Institute of Medical Science at the University of Tokyo, Tokyo, Japan; and [4]Center for Genome and Regenerative Medicine and [5]Atopy (Allergy) Center, Juntendo University School of Medicine, Tokyo, Japan

Key Points

- tPA expands mesenchymal stromal cells (MSCs) in the bone marrow by a cytokine (KitL and PDGF-BB) crosstalk with endothelial cells.
- Pharmacologic inhibition of receptor tyrosine kinases (c-Kit and PDGFRα) impairs tPA-mediated MSC proliferation.

Tissue plasminogen activator (tPA), aside from its vascular fibrinolytic action, exerts various effects within the body, ranging from synaptic plasticity to control of cell fate. Here, we observed that by activating plasminogen and matrix metalloproteinase-9, tPA expands murine bone marrow–derived CD45$^-$TER119$^-$Sca-1$^+$PDGFRα$^+$ mesenchymal stromal cells (PαS-MSCs) in vivo through a crosstalk between PαS-MSCs and endothelial cells. Mechanistically, tPA induces the release of Kit ligand from PαS-MSCs, which activates c-Kit$^+$ endothelial cells to secrete MSC growth factors: platelet-derived growth factor-BB (PDGF-BB) and fibroblast growth factor 2 (FGF2). In synergy, FGF2 and PDGF-BB upregulate PDGFRα expression in PαS-MSCs, which ultimately leads to PαS-MSC expansion. These data show a novel mechanism by which the fibrinolytic system expands PαS-MSCs through a cytokine crosstalk between niche cells. (*Blood*. 2016;128(8): 1063-1075)

Introduction

The bone marrow (BM) microenvironment, or niche, consists of the extracellular matrix (ECM) and a plethora of stromal cells and soluble factors that provide signals controlling the fate of stem cells.

Mesenchymal stromal cells (MSCs) constitute a crucial subset of BM stromal cells.[1] They are plastic-adherent multipotent cells, characterized by their ability to give rise to colony-forming unit-fibroblasts (CFU-Fs) and to differentiate into osteogenic, adipogenic, and chondrogenic lineages.[2-5] Aside from the BM, MSCs exist in various connective tissues such as fat,[6] muscle,[7] skin,[8] and placenta.[9] They make up 0.001% to 0.01% of human adult BM cells[10] and can be localized in perivascular spaces.[11] MSCs are defined by nonexpression of hematopoietic and endothelial markers like CD45, Ter119, and CD31 and expression of mesenchymal markers like CD146 for human BM-MSCs[12] or Nestin,[13] Leptin receptor,[14] platelet-derived growth factor receptor α (PDGFRα), and stem cell antigen-1 (Sca-1) for mouse MSCs.[15] As recently reviewed, these markers define distinct but overlapping subsets of MSCs.[16]

Proteases like the fibrinolytic factor plasmin and matrix metalloproteinase-9 (MMP-9) are upregulated within BM niche cells after myelosuppression.[17,18] Plasmin is generated by cleavage of the proenzyme plasminogen (Plg) by urokinase-type plasminogen activator (uPA) or tissue-type plasminogen activator (tPA). Activation of plasmin or MMPs cannot only accelerate local ECM degradation but can also lead to the activation/inactivation of chemo-/cytokines, receptors, and other proteases.[19,20] Mice deficient in membrane type 1 MMP show a decrease in the number of CD45$^-$Ter119$^-$Sca-1$^+$PDGFRα$^+$ cells (PαS-MSCs) and Nestin$^+$ MSCs within the BM.[21] Because the fibrinolytic factor plasmin can enhance the conversion of pro-MMPs to active MMPs, we reasoned that fibrinolytic factors might alter the cell fate of PαS-MSCs.

Here, we provide evidence that tPA induces the expansion of PαS-MSCs in part through Plg and MMP-9 activation. By blocking the c-Kit signaling pathway, we demonstrate that KitL released after tPA treatment is necessary for PαS-MSC propagation. KitL enhances the release of PDGF-BB and FGF2 from endothelial cells (ECs). These cytokines lead to the activation and upregulation of PDGFRα expression in PαS-MSCs. Although we have shown the importance of PDGFR and c-Kit signaling for tPA's effect on PαS-MSCs, potential contributions of other pathways cannot be excluded. Our data show a novel function of tPA in orchestrating a crosstalk between PαS-MSCs and ECs, leading to PαS-MSC expansion.

Materials and methods

Experimental animals

All procedures were approved by the Experimental Animal Care and Use Committee in the Animal Review Board of Institute of Medical Science,

Submitted October 1, 2015; accepted May 27, 2016. Prepublished online as *Blood* First Edition paper, June 9, 2016; DOI 10.1182/blood-2015-10-673103.

*K.H. and B.H. share senior coauthorship.

The online version of this article contains a data supplement.

There is an Inside *Blood* Commentary on this article in this issue.

The publication costs of this article were defrayed in part by page charge payment. Therefore, and solely to indicate this fact, this article is hereby marked "advertisement" in accordance with 18 USC section 1734.

University of Tokyo. Wild-type C57BL/6 (WT B6) mice were purchased from SLC. *tPA*$^{-/-}$, *Plg*$^{-/-}$, plasminogen activator inhibitor-1 (*PAI-1*)$^{-/-}$, and *MMP9*$^{-/-}$ were also on a WT B6 background.

In vivo treatment

WT B6 mice were treated with recombinant serpin-resistant tPA (provided by Eisai, Tokyo, Japan) at high dose (correlating to dosage used in humans) using 31 250 IU (250 μg/157 μL) per mouse (25 g body weight) at days 0 and 1 or with control solvent phosphate-buffered saline (PBS). Low-dose tPA was injected intraperitoneally at 27 500 IU/kg daily from days 0 to 7. uPA (Wakamoto; UKD43B1) was injected intraperitoneally for 2 to 5 days at 1 μg/kg.

Mice were treated at day 0 with 5-fluorouracil (5-FU; 250 mg/kg); neutralizing c-Kit antibody ACK2 (clone ASK; provided by Dr Shin-ichi Nishikawa, Riken, Kobe; 125 μg/mouse) every other day; recombinant murine SCF (KitL; Peprotech; 2.5 μg/mouse) from days 0 to 1; Gleevec (LC Laboratories; imatinib nethanesulfonate salt 99%; 100 mg/kg); and/or fibroblast growth factor (FGF) receptor inhibitor (LC Laboratories; PD173074; 2 mg/kg) daily. Epidermal growth factor receptor (EGFR) inhibitor erbitux (Cetuximab; 7.5 mg/kg) and PDGFR inhibitor Crenolanib (Selleck Chemicals; 22 mg/kg) were given at day 0 prior to tPA injection.

Preparation of PαS-MSCs

As previously described,[15] crushed femurs were incubated with gentle shaking for 1 hour at 37°C in Dulbecco's modified Eagle medium Dulbecco's modified Eagle medium (Invitrogen)/0.2% collagenase (Wako Chemicals). Cell suspension was filtered with a 70-μm cell strainer (BD Falcon). The cell pellet was resuspended in 1 mL sterile water (Sigma-Aldrich) for 5 to 10 seconds to burst the red blood cells, after which 1 mL of 2× PBS/4% fetal bovine serum (FBS) was added. Single cells were suspended in ice-cold Hanks balanced salt solution/2% FBS (2-3 × 10^7 cells/mL) and stained for 30 minutes with the following monoclonal antibodies (mAbs): allophycocyanin-conjugated PDGFRα (APA5), fluorescein isothiocyanate (FITC)-conjugated Sca-1 (Ly6A/E), Pacific blue–conjugated CD45 (30-F11), PE-TER119 (TER-119), FITC-conjugated CD31 (PECAM-1), and biotinylated LeptinR (R&D Systems; BAF497). Unless otherwise indicated, all mAbs were purchased from eBioscience. Biotinylated antibodies were visualized with allophycocyanin-conjugated streptavidin (Invitrogen). Flow cytometry was performed on a fluorescence-activated cell sorter (FACS) Verse and Aria (BD Biosciences) flow cytometer. Femoral muscle and subcutaneous fat were similarly collagenase digested, and single cells were stained for PαS-MSC markers.

Cell cycle analysis

PαS-MSCs were suspended in warm medium at 10^6 cells/mL and mixed with Hoechst 33342 (Dojindo) at 10 μg/mL. Verapamil was added at 40 μg/mL to block dye flux. Cells were incubated for 40 minutes at 37°C with occasional shaking. Pyronin Y (Sigma-Aldrich) was added at 0.5 μg/mL. Cells were incubated for 20 minutes, centrifuged, and resuspended in FACS buffer for subsequent analysis.

Cell culture

Primary cell cultures. FACS-isolated murine PαS-MSCs, murine magnetic-activated cell sorting–sorted $CD45^-CD31^+$ ECs, or human umbilical vein endothelial cells (HUVECs) were cultured at 37°C/5% CO_2 on 0.1% gelatin (Wako Pure Chemicals)-coated culture plates (Falcon) in MSC growth medium (minimum essential medium-α GlutaMAX and 10% FBS; Gibco) or endothelial growth medium-2 (EGM-2; Lonza; cc4176), respectively. The T17B cell line was cultured in Dulbecco's modified Eagle medium/10% FBS.

Transwell cocultures. PαS-MSCs were seeded into the lower chamber of a transwell plate (Corning) in growth medium. ECs were seeded in the upper chamber precoated with 0.1% gelatin using a 0.4-μm pore-sized transwell in EGM-2 medium. Cells were left to adhere overnight, then cocultured in EBM-2/ 2% FBS medium for 3 days. tPA (5 μg/mL), ACK-2 (2 μg/mL), Gleevec (5 μM), or PDGFRα inhibitor Crenolanib (Selleck Chemicals; 0.5 μg/mL) were added daily.

Cytokine-supplemented cultures. PαS-MSCs were treated with bovine serum albumin (BSA), tPA (Eisai; 5 μg/mL), PDGF-AA/-BB/-DD (Peprotech; 10 ng/mL), PDGF-CC (R&D Systems; 100 ng/mL), FGF2 (Peprotech; 1 ng/mL), or EGF (Santa Cruz Biotech; 20 ng/mL). ECs (isolated from mouse or HUVECs) were treated with BSA, tPA (Eisai, 5 μg/mL), and KitL (Peprotech; 10 ng/mL). Inhibitors were added daily: Gleevec (5 μM), ACK-2 (2 μg/mL), and MMP inhibitor MMI270 (Novartis; 1 μM).

CFU-F assay

Single cells were cultured in MSC growth medium in 96-well plates. Adherent visible colonies (>50 cells) are counted after 14 days.

Cell proliferation assay

Freshly isolated murine PαS-MSCs (5000 cells per well) were cultured in triplicate for 3 days in a 96-well plate with MSC growth medium. Cell Counting Kit-8 was used according to the manufacturer's recommendations (Dojin-Wako Pure Chemical). Absorbance was measured at 450 nm by an enzyme-linked immunosorbent assay (ELISA) plate reader (Molecular Devices; microplate reader with SoftMax Pro).

For the 5-bromo-2′-deoxyuridine (BrdU) assay, FACS-sorted PαS-MSCs derived from control and tPA-treated mice were analyzed using BrdU Cellomics proliferation kit (Thermo Scientific). Cells were fixed, permeabilized, and stained according to the manufacturer's instructions. Ten images per group were analyzed using a fluorescent microscope.

Quantitative reverse transcriptase–polymerase chain reaction analysis

Total RNA was prepared using TRIzol Reagent (Ambion by Life Technologies; 15596018) according to the manufacturer's instructions. First-strand cDNA was synthesized from 0.2 to 2 μg of total RNA using a High Capacity Reverse Transcriptase kit (Applied Biosystems) run using a quantitative polymerase chain reaction (qPCR) machine Step One Plus (Applied Biosystems) with SYBR Premix Ex Taq II (×2) Tli RNaseH Plus (Takara; #RR820). Primer sequences are provided in supplemental Table 1, available on the *Blood* Web site.

ELISA

Serum/plasma were used for ELISA of mouse PDGF-BB and KitL (R&D Systems) according to the manufacturer's protocol.

Western blot analysis

Cultured PαS-MSCs were lysed with ice-cold cell lysis buffer. Conditioned medium was centrifuged at 15 000 rpm for 10 minutes at 4°C, and supernatants were collected. Crude protein was recovered by ice-cold acetone. Cell lysates (2- to 50-μg proteins) were applied on an 8% or 10% acrylamide gel, transferred to polyvinylidene fluoride membrane (Millipore; Immobilon), blocked, and then stained overnight at 4°C for PDGFRα (Abcam; ab61219), PDGFRβ (Cell Signaling; 3169), PDGF-BB (Santa Cruz Biotech; sc-7878), KitL (Santa Cruz Biotech; sc-9132), FGF2 (Santa Cruz Biotech; sc-79), α-actinin (Santa Cruz Biotech; sc-17829), α/β tubulin (Cell Signaling; 2148), p-PDGFRα/Tyr 720 (Santa Cruz Biotech; sc-12910), or PDGFRβ-PY1021 (Cell Signaling; 2227). Membranes were stained with secondary antibody conjugated with horseradish peroxidase (HRP; Nichirei; rabbit-HRP or goat-HRP), and developed with the ECL Plus detection system (Amersham Life Science; RPN2132) using the image analyzer Image-Quant LAS4000 (GE Healthcare).

Receptor tyrosine kinase array

tPA-treated and control PαS-MSCs (5 × 10^4 cells per 6-well plate), cultured for 1 day, were analyzed using the receptor tyrosine kinase (RTK) array kit (R&D Systems; #ARY014) according to the manufacturer's protocol. The band intensity was measured using an Epson scanner and analyzed using image analysis software (ImageJ; National Institutes of Health).

Gelatin-based zymography

Zymography was performed as previously described.[22] The density of each lytic band was quantified using ImageJ. See supplemental Data.

Immunohistochemistry

Mouse femurs were snap frozen with Tissue-Tek OCT Compound (Sakura) in liquid nitrogen. Tissue sections were blocked and stained with primary antibodies overnight at 4°C: PDGFRα (Abcam; ab61219 and Santa Cruz Biotech; sc-431), KitL (Santa Cruz Biotech; sc-9132), VE-Cadherin (BD Pharmingen; 550548), Nestin (Abcam; Ab6142), PDGF-BB (Santa Cruz Biotech; sc-7878), FGF-2 (Santa Cruz Biotech; sc-79), c-Kit (Santa Cruz Biotech; sc-168), and respective mouse, rat, and rabbit immunoglobulin (Ig)G (Santa Cruz Biotech) controls followed by Alexa488- or Alexa594-conjugated secondary antibodies (IgG H+L) (Invitrogen; A11072 and A11017). Nuclei were counterstained with 4′,6-diamidino-2-phenylindole (DAPI; Molecular Probes). Images were taken with Olympus fluorescence microscopes IX71 and BX51 using an Olympus DP72 camera.

Statistical analysis

Results are presented as means ± standard error of the mean (SEM). *P* values were calculated by Student *t* test or analysis of variance (ANOVA) with Tukey honest significant difference (HSD) post hoc tests using the R program for multigroup analysis.

Results

tPA expands CD45$^-$Ter119$^-$Sca-1$^+$PDGFRα$^+$ MSCs in mice

Components of the fibrinolytic cascade, including the uPA receptor (uPAR) and PAI-1 are expressed in MSCs,[1] but the role of fibrinolytic factors in MSC maintenance is not well understood. In this study, we took advantage of homozygous knockout mice for the Plg, tPA, and PAI-1 genes. We observed a higher frequency of PαS-MSCs in the BM of PAI-1$^{-/-}$ compared with WT B6 mice under steady-state conditions (Figure 1A).

Administration of tPA according to the scheme shown in Figure 1B increased the frequency and absolute numbers of PαS-MSCs. Even at a lower dose, tPA treatment incrementally expanded BM PαS-MSCs (supplemental Figure 1A). PαS-MSCs also stained positive for the MSC-associated marker Nestin (Figure 1C). tPA treatment similarly increased the percentage of CD45$^-$Ter119$^-$CD31$^-$LeptinR$^+$ MSCs in the BM (Figure 1D), indicating that tPA treatment expanded various MSC subtypes.[16]

PαS-MSCs isolated 2 days after tPA injection (tPA-MSCs), showed a higher proliferation rate (Figure 1E-G) and gave rise to more CFU-s) in liquid culture (Figure 1H) compared with control PαS-MSCs.

Both tPA- and control PαS-MSCs cultured in differentiation medium exhibited multilineage differentiation into Oil red O$^+$ adipocytes, Alizarin red$^+$ osteoblasts, and Toluidine blue$^+$ chondrocytes (supplemental Figure 1B) and showed upregulation of some of the tested adipocytic (PPAR-γ2, aP2, Adipsin), osteoblastic (Runx2, Osterix, osteocalcin), and chondrocytic (COL2A1, COL10A1, Aggrecan) differentiation genes (supplemental Figure 1C).

tPA administration systemically activates the fibrinolytic system and might alter the frequency of PαS-MSCs in other tissues. Aside from the BM, the number of PαS-MSCs also increased in subcutaneous abdominal white fat and muscle tissues after tPA administration (Figure 1I). Together, these data suggest that tPA expands multipotent PαS-MSCs with colony-forming and mesenchymal lineage differentiation ability in various MSC niches.

tPA-mediated PαS-MSC expansion is impaired in Plg$^{-/-}$ and MMP-9$^{-/-}$ mice

Plasmin is generated by tPA- or uPA-mediated conversion of plasminogen. Plasmin can activate MMPs like MMP-2 and MMP-9.[18,23,24] tPA- and uPA-injected mice showed higher plasma levels of active MMP-2, MMP-9, and plasmin compared with control mice (supplemental Figure 2A-B). However, the frequency of PαS-MSCs in BM at 2 (supplemental Figure 2C) or 5 days (data not shown) did not change in uPA-injected mice. tPA-mediated MSC expansion did not occur in Plg$^{-/-}$ or MMP-9$^{-/-}$ mice (Figure 2A-B), indicating that plasmin and MMP-9 activation is important for tPA-driven PαS-MSC expansion. These data indicate that aside from protease activation, tPA but not uPA, expands PαS-MSCs by activating other MSC signaling molecules.

MSC growth factors are upregulated in the BM following tPA administration

Proteases like plasmin, MMPs, or tPA might expand MSCs by changing the bioavailability of growth factors.[1,18,25-27] Several growth factors can expand MSCs, but only a few of these can also be activated by fibrinolytic factors. We focused on these growth factors and screened their expression in BM mononuclear cells (BMNCs) of tPA-treated or control mice. Furthermore, we included some MSC growth factors recently reported to play a role in the proliferation and differentiation of BM-derived MSCs[28]: platelet growth factor-A (PDGFA), PDGFC, PDGFB, and PDGFD, vascular endothelial growth factor, transforming growth factor β 1 (TGFβ1), epidermal growth factor (EGF), insulin-like growth factor-1, hepatocyte growth factor, FGF2, bone morphogenetic protein-2 (BMP-2), and BMP-3. *PDGF-BB*, *EGF*, and *FGF2* expression was the highest in BMNCs derived from tPA-treated compared with vehicle-treated mice (Figure 2C). EGFR signaling protects MSC-like cells from FasL-induced apoptosis.[29] Both recombinant (rec.) PDGF-BB and FGF-2, but not EGF, expanded PαS-MSCs in vitro (Figure 2D). Increased PDGF-BB plasma levels were detected only in tPA-treated WT B6 and tPA$^{-/-}$, but not in Plg$^{-/-}$ or MMP-9$^{-/-}$ mice (Figure 2E).

It has been reported that FGF2 expands Nestin$^+$ stromal cells/MSCs and enhances c-Kit/KitL signaling in hematopoietic progenitors within the BM.[30] Next, we asked whether FGF2 can amplify KitL signaling in PαS-MSCs. PαS-MSCs treated with tPA or FGF2 showed high KitL expression (Figure 2F), and high KitL expression was also detectable in perivascular PDGFRα$^+$ cells in immunostained BM sections (Figure 2G). Increased KitL plasma levels were found in tPA-injected mice (Figure 2H). These data suggest that tPA might expand PαS-MSCs in vivo by enhancing the expression of KitL from PαS-MSCs, but possibly also from other stromal cells. Our data are consistent with previous reports demonstrating enhanced release of KitL from stromal cells.[18]

KitL restores impaired tPA-mediated PαS-MSC expansion in Plg$^{-/-}$ and MMP-9$^{-/-}$ mice

MMP activation is required for tPA-mediated release of KitL from stromal cells.[18] To determine whether the tPA-mediated release of KitL from PαS-MSCs was dependent on the activation of MMP-2 and -9, we treated PαS-MSCs with tPA in the absence or presence of MMP inhibitor. tPA-treated PαS-MSCs secreted more active MMP-2 and MMP-9 (Figure 3A-B), and tPA-mediated release of KitL from MSCs was downregulated in the presence of an MMP inhibitor (Figure 3C). In agreement with

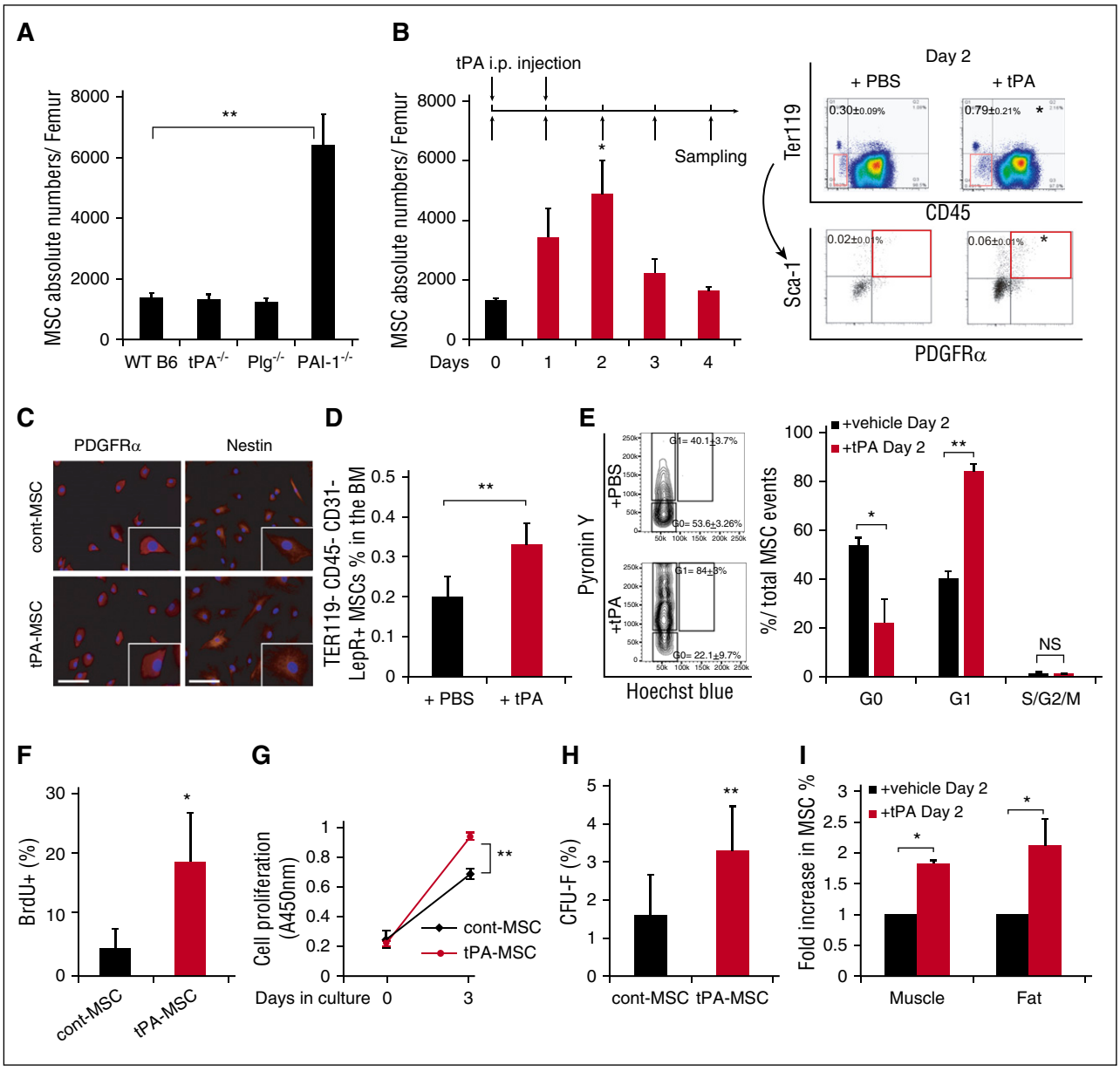

Figure 1. Tissue-type plasminogen activator expands CD45$^-$Ter119$^-$Sca-1$^+$PDGFRα$^+$ MSCs in mice. C57BL/6 (WT B6) mice were injected daily intraperitoneally with a serpine-resistant recombinant tissue tPA on day 0 and day 1. MSCs were identified using the following marker profile: CD45$^-$Ter119$^-$Sca-1$^+$PDGFRα$^+$ (PαS-MSCs) by FACS. (A) Absolute numbers of PαS-MSCs per femur in WT B6 and tPA$^{-/-}$, Plg$^{-/-}$, and PAI-1$^{-/-}$ BM cells under steady state as determined by FACS (n = 3-4/group). (B) Absolute numbers of MSCs per femur from tPA-treated or PBS-treated WT B6 mice following the indicated treatment schedule as determined by FACS analysis (n = 5/group; left). FACS gating schedule shown (right). (C) Immunohistologic staining for Nestin in ex vivo cultured MSCs derived from tPA and vehicle-treated mice. Nuclei were counterstained using DAPI (n = 3/group). Scale bars, 20 μm. (D) The percentage of CD45$^-$Ter119$^-$CD31$^-$LeptinR$^+$ MSCs in BM cells of tPA-treated or PBS-treated WT B6 mice as determined by FACS (n = 3/group). (E) Cell cycle analysis from freshly isolated PαS-MSCs derived from tPA and control BM cells (n = 3-4/group). (F) BrdU cell proliferation assay was performed using PαS-MSCs derived from mice treated with/without tPA (n = 4 /group). (G) Using the colorimetric cell counting kit-8, the relative absorbance at 450 nm as a measure for cell proliferation is given for PαS-MSCs derived from control or tPA-treated mice (n = 3/group). (H) Freshly isolated PαS-MSCs from tPA or PBS-treated WT B6 mice were grown as single cell cultures for 14 days. The number of CFU-F was counted (n = 2000/group). (I) The percentage of PαS-MSCs in femoral muscle and subcutaneous white fat isolated from tPA- or PBS-treated WT B6 mice on day 2 is indicated as determined by FACS (n = 4/group). Mean ± SEM. *$P < .05$; **$P < .01$; ***$P < .001$ by Student t test. Data are representative of 2 independent experiments.

reports by others, we found that PαS-MSCs do not express the KitL receptor, c-Kit (Figure 3D),[15] and recombinant KitL failed to expand PαS-MSCs in vitro (Figure 3E). These data imply that KitL does not enhance PαS-MSC expansion in an autocrine manner. However, administration of recombinant KitL in mice increased the absolute numbers of WT, *Plg*$^{-/-}$, and *MMP-9*$^{-/-}$ BM PαS-MSCs (Figure 3F-G). By contrast, the ACK2 neutralizing antibody against c-Kit prevented tPA-mediated PαS-MSC expansion (Figure 3H). These data suggest that tPA expands PαS-MSCs in vivo by enhancing the expression of KitL from c-Kit- PαS-MSCs.

EC-derived PDGF-BB and FGF2 enhance PαS-MSC expansion

Because our evidence suggested a role for the c-Kit/KitL pathway in tPA-mediated MSC expansion, we asked which c-Kit$^+$ cells might mediate the activation of this pathway. We

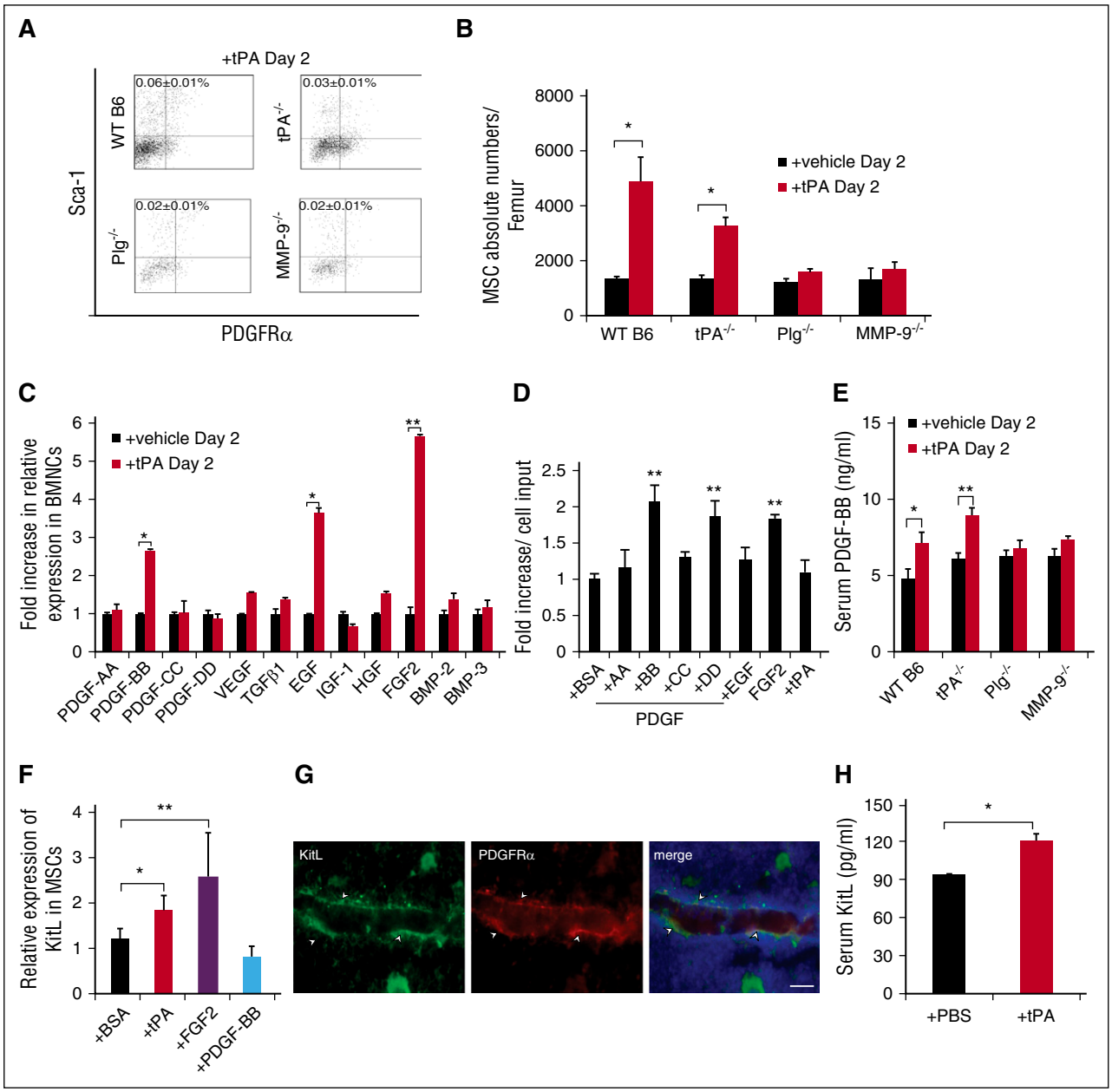

Figure 2. tPA expands PαS-MSCs in a Plg- and MMP-9–dependent manner and results in the activation of MSC growth factors. (A) Representative FACS blots and (B) the absolute numbers of PαS-MSCs per femur from WT B6 mice, *Plg*$^{-/-}$, *MMP-9*$^{-/-}$, and *tPA*$^{-/-}$ mice treated for 2 days with recombinant tPA or vehicle as determined by FACS analysis (n = 3/group). (C) Expression of genes involved in MSC maintenance/proliferation: platelet derived growth factor-A, PDGF-BB, PDGF-CC, PDGF-DD, vascular endothelial growth factor, TGFβ1, eEGF, insulin-like growth factor-1, hepatocyte growth factor, FGF2, BMP-2, and BMP-3 in total BMNCs retrieved from rec. tPA or vehicle-treated mice at day 2. The mRNA levels are standardized to glyceraldehyde-3-phosphate dehydrogenase (GAPDH; n = 3/group). (D) Fold increase of the number of cultured PαS-MSCs compared with initial cell input after treatment with recombinant PDGF-AA, PDGF-BB, PDGF-CC, PDGF-DD, EGF, FGF2, and tPA for 3 days (n = 3/group). (E) PDGF-BB serum level was measured by ELISA on day 2 from tPA-treated WT B6, *tPA*$^{-/-}$, *Plg*$^{-/-}$, and *MMP-9*$^{-/-}$ mice (n = 3/group). (F) Relative mRNA expression of KitL in MSCs (P4) cultured in the presence of vehicle, tPA, FGF2, and PDGF-BB for 2 days. Data are normalized to GAPDH (n = 4/group). (G) Immunohistologic staining for KitL (green) and PDGFRα (red) in BM sections of tPA-treated mice. Arrows indicates perivascularly localized PDGFRα^{+} KitL coexpressing cells. Scale bar, 10 μm. (H) Serum KitL levels of WT B6 mice treated with vehicle or rec. tPA for 2 days as determined by ELISA (n = 3/group). Mean ± SEM. *$P < .05$; **$P < .01$; ***$P < .001$ by Student *t* test or ANOVA with Tukey HSD tests for multigroup analysis. Data are representative of 2 independent experiments.

investigated the role of ECs as c-Kit^{+} mediator cells, because we had shown that tPA treatment increased the expression of angiocrine factors in BMNCs (Figure 2C) and that PαS-MSCs are perivascular[15] (Figure 4A). Consistent with the observed increase in CD45^{-}Ter119^{-} cells in tPA-treated BM (Figure 1B), we found more VE-Cadherin^{+} ECs compared with vehicle-treated BM (Figure 4B). These results indicate that tPA augments the numbers of 2 important stromal cell types in the BM niche: PαS-MSCs and VE-Cadherin^{+} ECs.

Indeed, immunoreactive PDGF-BB and FGF2 signals were observed in VE-Cadherin^{+} ECs in BM sections from tPA-treated mice (Figure 4C-D). Higher PDGF-BB and FGF2 gene expression was found in CD45^{-}CD31^{+} ECs isolated from tPA-treated, but not from vehicle-treated, mice (Figure 4E).

c-Kit neutralizing antibody (ACK2) administration prevented the tPA-mediated increase in PDGF-BB plasma levels (Figure 4F). Injection of recombinant KitL restored PDGF-BB serum release after tPA treatment in Plg$^{-/-}$ and MMP-9$^{-/-}$ mice (Figure 4G).

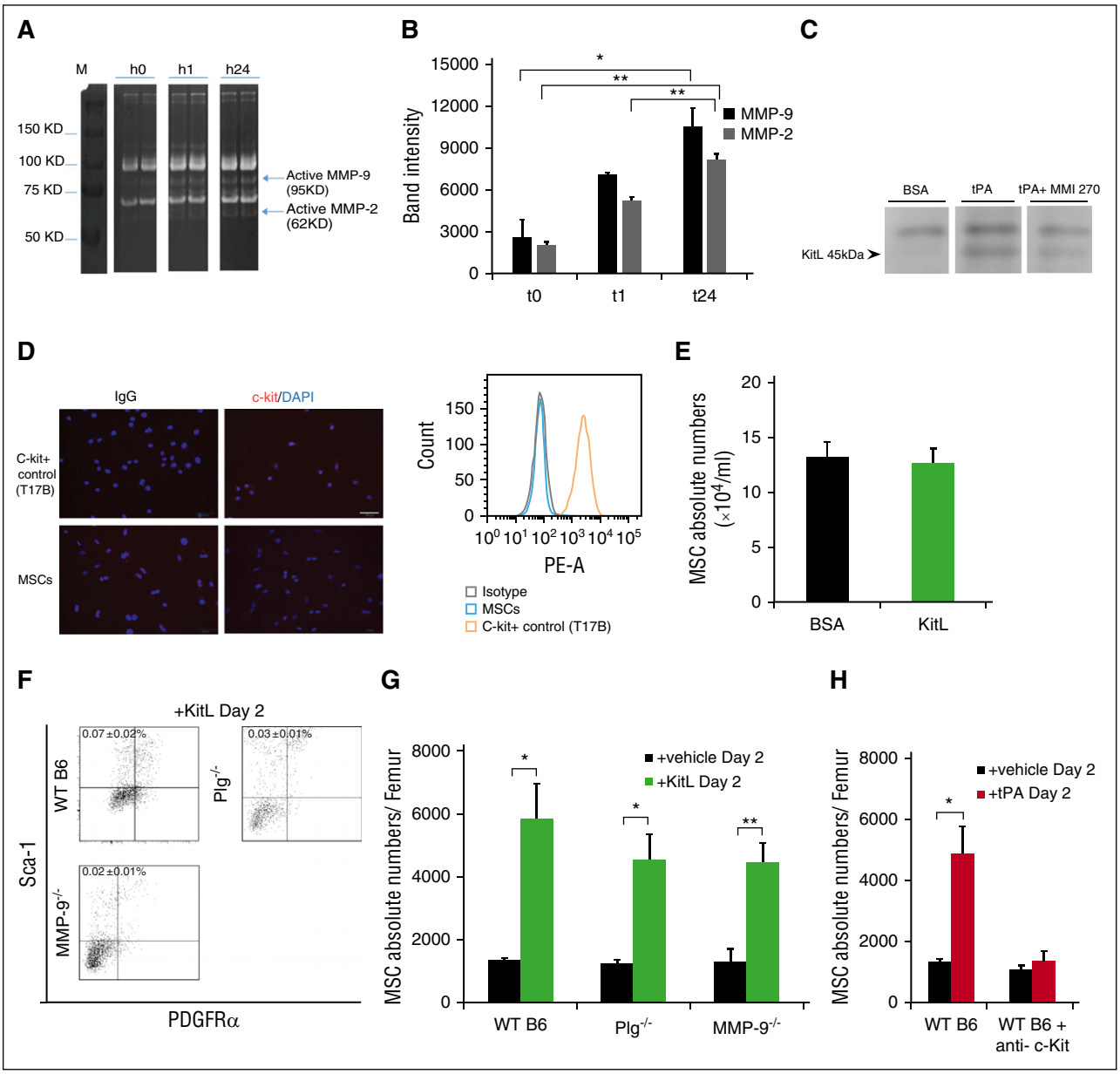

Figure 3. KitL restores impaired tPA-mediated PαS-MSC expansion in Plg$^{-/-}$ and MMP-9$^{-/-}$ mice. (A) Original gel and (B) densitometric quantification of MMP-2 and MMP-9 after gelatin zymography from supernatants derived from PαS-MSCs stimulated with/without tPA at indicated time points (n = 3/group). (C) Representative western blot of soluble KitL released in supernatant of cultured PαS-MSCs treated with vehicle or tPA with or without the MMP inhibitor MMI 270 (n = 3/group). (D) Immunohistologic staining (left) and FACS plot (right) for c-Kit expression in ex vivo cultured PαS-MSCs. T17B was used as a positive control. Nuclei were counterstained using DAPI (n = 3/group). Scale bars, 50 μm. (E) Absolute numbers of cultured PαS-MSCs per well after addition of rec. KitL or vehicle for 4 days as determined by hemocytometer counting (n = 3/group). (F) Representative FACS blots and (G) the absolute numbers of PαS-MSCs per femur from WT B6, *Plg*$^{-/-}$, and *MMP-9*$^{-/-}$ mice after 2 days of injection of rec. KitL or vehicle as determined by FACS analysis (n = 3/group). (H) Absolute numbers of PαS-MSCs per femur from WT B6 mice treated for 2 days with rec. tPA in the absence and presence of neutralizing c-Kit antibody. For comparison, WT B6 data of Figure 2B are used for reference (n = 4/group). Mean ± SEM. *$P < .05$; **$P < .01$; ***$P < .001$ by Student *t* test. Data are representative of 2 independent experiments.

These data indicate that tPA, in part through plasmin and MMP-9, enhances KitL release, which in turn can induce PDGF-BB expression in vivo. We also observed enhanced FGF2 and PDGF-BB gene expression in KitL- and tPA-treated mouse CD45^{-} CD31^{+} ECs (Figure 4H-I) or HUVECs (data not shown). The importance of c-Kit signaling for FGF2 and PDGF-BB release from ECs was further demonstrated by showing ACK2 impaired the secretion of FGF2 and PDGF-BB into the supernatant of KitL-treated HUVECs (Figure 4J). Moreover, tPA cotreatment with KitL and ACK2 rescued HUVEC secretion of PDGF-BB only and not secretion of FGF2. These data indicate that tPA induces PDGF-BB in a KitL-independent manner, but requires KitL signaling for FGF2 induction in ECs. PDGF-BB and FGF2 in turn activate PαS-MSCs to secrete more KitL, thereby creating an amplification loop.

FGF2 and PDGF-BB augment PDGFRα expression in PαS-MSCs

Various growth factor receptors on MSCs can enhance self-renewal and proliferation.[31] To determine which RTK is mainly activated on tPA-treated PαS-MSCs, an RTK assay was performed.

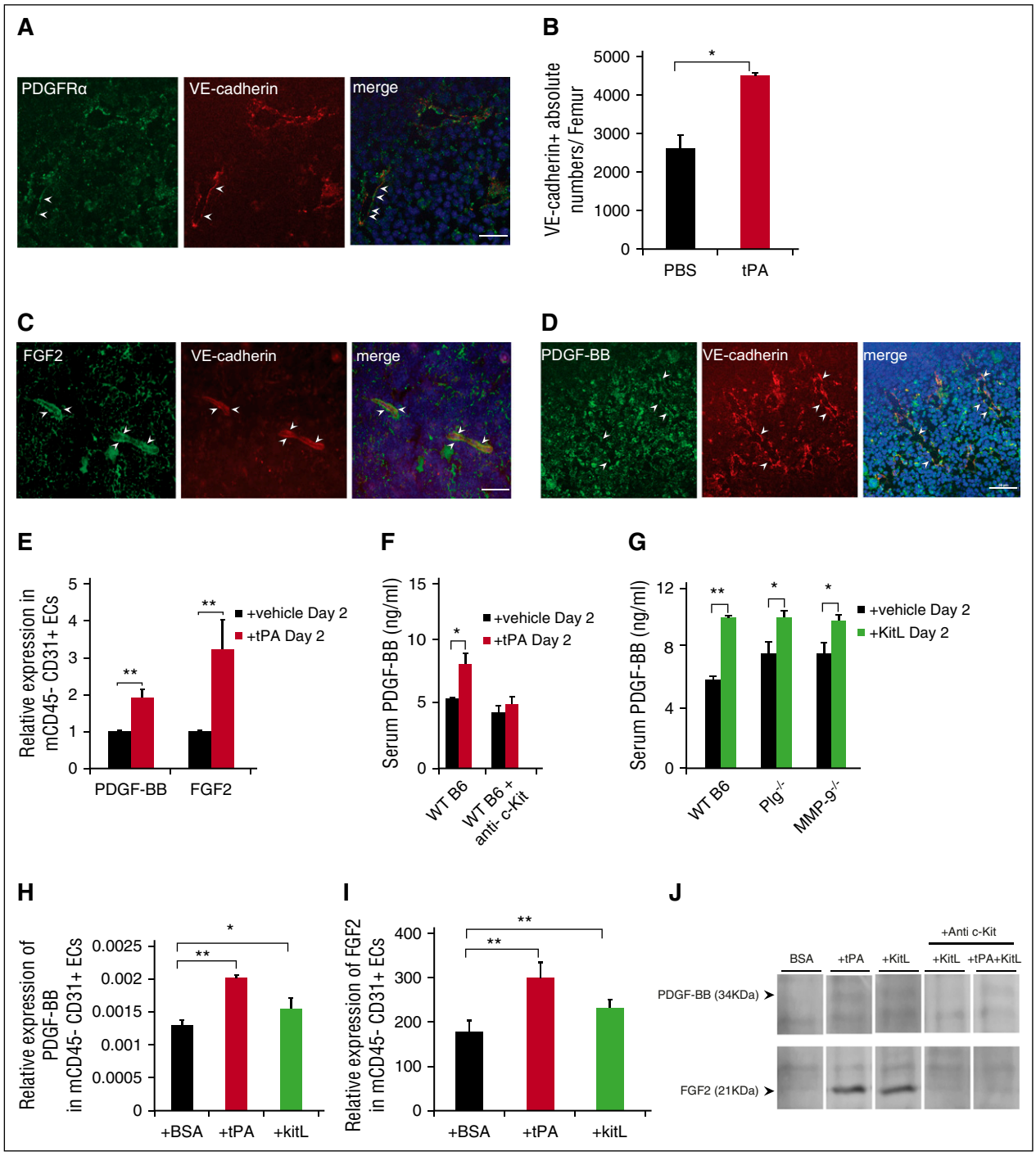

Figure 4. EC-derived PDGF-BB and FGF2 expand PαS-MSCs. (A) Immunohistologic staining for PDGFRα (green) and VE-Cadherin (red) in BM sections of tPA-treated mice. Scale bar, 50 μm. (B) Absolute numbers of VE-Cadherin$^+$ ECs per femur from WT B6 mice after 2 days of injection with recombinant tPA or vehicle was determined by FACS analysis (n = 3/group). (C-D) Representative images of (C) FGF2 and (D) PDGF-BB in BM sections of tPA-treated mice. Nuclei were counterstained using DAPI. VE-Cadherin (red) and FGF2/PDGF-BB (green). Arrows indicate FGF2 or PDGF-BB coexpressing BM-ECs after tPA treatment. Scale bar, 50 μm. Staining was repeated 4 times. (E) Relative mRNA expression of PDGF-BB and FGF2 in CD45$^-$CD31$^+$ ECs isolated from tPA and vehicle-treated mice. Data are normalized to GAPDH (n = 3/group). (F-G) PDGF-BB serum level was measured by ELISA on day 2 of (F) tPA treatment of WT B6 mice in the presence or absence of c-Kit neutralizing antibody or of (G) KitL treatment of WT B6, *Plg*$^{-/-}$, and *MMP-9*$^{-/-}$ mice. Same control from Figure 2E was used for reference (n = 3/group). (H-I) Relative mRNA expression of (H) PDGF-BB and (I) FGF2 as determined by reverse transcriptase (RT)-PCR in CD45$^-$CD31$^+$ ECs treated with vehicle, tPA, or KitL for 2 days. Data are normalized to GAPDH (n = 6/group). (J) Representative western blot of PDGF-BB and FGF2 in supernatant of HUVECs treated in vitro with vehicle, tPA, and KitL with or without c-Kit neutralizing antibody, ACK2 (n = 3/group). Mean ± SEM. *$P < .05$; **$P < .01$; ***$P < .001$ by Student *t* test or ANOVA with Tukey HSD tests for multigroup analysis.. Data are representative of 2 independent experiments.

Higher phosphorylation of PDGFRα was found in tPA-MSCs compared with control MSCs (Figure 5A) and was confirmed by western blotting (Figure 5B). No difference between tPA-treated and control MSCs was found for other tested RTKs.

Next, we investigated the ability of FGF2 and PDGF-BB to alter PDGFRα expression on PαS-MSCs. FGF2 augmented PDGFRα, but not PDGFRβ, expression on PαS-MSCs in a dose-dependent manner at the transcriptional (Figure 5C-D) and the protein levels (Figure 5E-F).

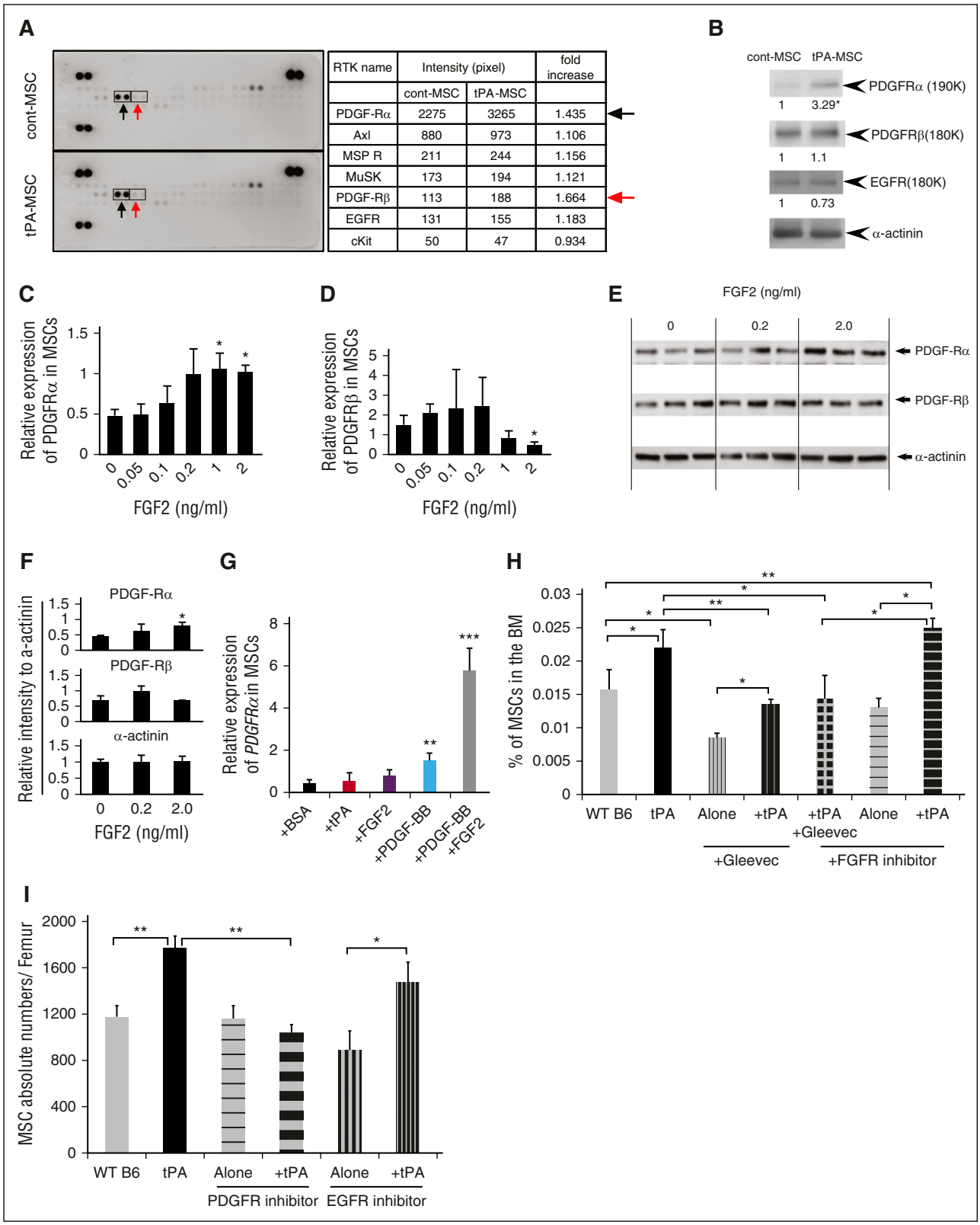

Figure 5. FGF2 and PDGF-BB augment PDGFRα expression in PαS-MSCs. (A) Whole-cell extracts of ex vivo–cultured PαS-MSCs derived from vehicle or tPA-treated mice were incubated on mouse receptor tyrosine kinase-phosphorylation antibody array, and phosphorylation status was determined by subsequent incubation with HRP-conjugated antiphosphotyrosine (each RTK spotted in duplicate, positive controls in corners, gene identity in the right panel). Increased tyrosine phosphorylation for PDGFRα (black arrow) and PDGFRβ (red arrow) is shown (n = 2/group). (B) Representative western blot of PDGFRα and PDGFRβ and EGF receptor in cell lysates of cultured PαS-MSCs derived from control PBS- or tPA-treated mice (n = 3/group). α-Actinin was used as a loading control. (C-D) Relative mRNA expression of (C) PDGFRα and (D) PDGFRβ in cultured PαS-MSCs stimulated with recombinant FGF2 at indicated concentrations for 18 hours in serum-reduced medium as determined by RT-PCR. Data are normalized to GAPDH (n = 3/group). (E-F) Relative protein expression of PDGF-Rα and PDGFRβ in PαS-MSCs stimulated with recombinant FGF2 at indicated concentrations for 18 hours in serum-reduced medium as determined by western blot analysis. Relative intensity of each band was measured and normalized to α-actinin

PDGFRα gene expression on cultured PαS-MSCs was slightly induced by PDGF-BB alone but was strongly induced in synergy with FGF2 (Figure 5G). Coinjection studies show that the general RTK inhibitor Gleevec and a specific PDGFRα inhibitor blocked tPA-mediated PαS-MSC expansion in WT B6 mice, but a specific FGFR inhibitor or EGFR inhibitor did not (Figure 5H-I). These data underscore the importance of c-Kit and PDGFR signaling for tPA-mediated PαS-MSC expansion in vivo.

PDGFRα and c-Kit blockade prevents tPA-induced PαS-MSC expansion in EC and PαS-MSC cocultures

To further investigate the cytokine crosstalk between PαS-MSCs and ECs, we established an MSC–EC coculture system (Figure 6A). HUVECs (Figure 6B) or magnetic-activated cell sorting–isolated murine $CD45^{-}CD31^{+}$ ECs (Figure 6C) were cocultured with murine PαS-MSCs in the presence or absence of recombinant tPA. Cocultured PαS-MSCs showed a higher proliferation rate when tPA was added, a process driven by soluble factors as both cell types were separated by a transwell membrane during the culture. By choosing cells from different species, the coculture system allowed us to study which growth factor was released from which cell type. tPA addition increased PDGF-BB and FGF2 expression in human and mouse ECs (Figure 6D-E) and KitL or PDGFRα expression in PαS-MSCs (Figure 6F).

Activated MMP-2 and MMP-9 derived from PαS-MSCs were detected by zymography in tPA- but not BSA-supplemented coculture supernatants (Figure 6G-H). These data confirmed that tPA enhanced the secretion of PDGF-BB/FGF2 from ECs and induced MMP-2, MMP-9, KitL, and PDGFRα expression in PαS-MSCs in MSC-EC cocultures. We further confirmed that receptor inhibitors did not alter the proliferation of PαS-MSCs cultured in the absence of ECs (Figure 6I). The tPA-mediated PαS-MSC expansion in MSC-EC coculture could be prevented using c-Kit neutralizing antibody, a PDGFRα inhibitor, and a more general RTK inhibitor (Gleevec). These data indicate that c-Kit and PDGFRα signaling are important for tPA-mediated but not baseline PαS-MSC expansion in the presence of ECs (Figure 6J).

Fibrinolytic system regulates PαS-MSC expansion following myelosuppression

Protease activation occurs after myelosuppression as a stress response in the postnatal BM niche.[17,18] We previously reported high tPA expression in BM stroma cells following 5-FU treatment,[18] indicating that endogenous tPA might have a role in regulating the BM niche after myelosuppression. PαS-MSCs, as part of the BM stroma cell compartment, are quiescent cells in the G0 phase of the cell cycle[15] and thus resistant to 5-FU. 5-FU treatment increased BM PαS-MSCs numbers in WT B6 and PAI-$1^{-/-}$ mice by more than twofold. In contrast, the expansion of PαS-MSCs in $tPA^{-/-}$ mice was less prominent (Figure 7A). Coinjection of 5-FU with recombinant tPA rescued the impaired proliferation of PαS-MSCs in $tPA^{-/-}$ mice (Figure 7B). Fewer $tPA^{-/-}$ PαS-MSCs had entered the S/G2M phase of the cell cycle after 5-FU treatment, indicating that tPA is 1 factor driving PαS-MSC proliferation after myelosuppression (Figure 7C). Our data suggest that tPA is a stress response molecule important for BM niche remodeling after myelosuppression.[32]

Discussion

Although PαS-MSCs reside in the vicinity of ECs within the BM niche,[12] it is not well established how these cells communicate with each other. tPA is highly expressed in tissues during extensive tissue remodeling.[18,33,34] In this study, we show that tPA can expand PαS-MSCs by catalyzing a cytokine crosstalk between PαS-MSCs and c-Kit^{+} ECs involving the activation of the Plg/PA and the MMP proteolytic systems. We demonstrate that even though uPA and tPA augmented plasmin and active MMP plasma levels, only tPA expanded PαS-MSCs in vivo, a phenomenon known already for human smooth muscle cells.[35]

We show that tPA alone and tPA-induced KitL, but maybe as yet unidentified factors released from PαS-MSCs after tPA treatment augment PDGF-BB expression in c-Kit^{+} ECs. PDGF-BB, in synergy with FGF2, amplifies PDGFRα signaling in BM PαS-MSCs. Although in this study we mapped out the involvement of c-Kit/KitL and PDGF-BB/PDGFR signaling in tPA-mediated PαS-MSC expansion, there may well be other contributing pathways. Although FGF2 signaling was involved in tPA-mediated PαS-MSC expansion in vitro, the blockade of this pathway was not sufficient to suppress PαS-MSC expansion in vivo. The reason for this discrepancy between the in vitro and in vivo results is not clear and requires further studies. The tPA-induced cytokine crosstalk ultimately leads to PαS-MSC expansion in the BM and possibly other MSC niches. This is schematically represented in Figure 7D.

Consistent with our data on PDGFRα upregulation after FGF2 treatment of BM ECs, it was reported that FGF2 triggers PDGFRα expression at the transcriptional level in ECs within the tumor microenvironment. This makes ECs hyperresponsive to PDGF-BB, resulting in enhanced angiogenesis.[34,36] We showed that tPA increased both the number of VE-Cadherin^{+} EC and PαS-MSCs, but had a larger effect on PαS-MSCs, because it decreased the EC/PαS-MSC ratio in the BM from 2.8 to 1.5 (data not shown).

Fibrinolytic factors increase after chemotherapy or irradiation.[18,37] We observed that PαS-MSC expansion after myelosuppression depended partially on endogenous tPA. Host-derived BM-MSCs in BM transplant recipients survive radiation doses lethal to the hematopoietic system.[38,39] It is tempting to speculate that 1 function of the fibrinolytic factors following BM transplantation is to reset/replenish the cellular BM niche compartment that subsequently will drive donor HSC engraftment and hematopoietic recovery.

Among other factors, hematopoietic recovery after myelosuppression is dependent on KitL and protease (tPA/plasmin-mediated MMPs) activation.[17,21] Ding et al demonstrated that ECs and *LepR*-expressing perivascular stromal cells produce KitL.[40] We found that tPA, among other untested factors, can upregulate KitL expression in PαS-MSCs and that c-Kit/KitL signaling

Figure 5 (continued) (n = 3/group). (G) Relative mRNA expression of PDGFRα in cultured PαS-MSCs treated for 2 days with PBS, tPA, FGF2, PDGF-BB, or FGF2 and PDGF-BB as determined by RT-PCR. Data are normalized to GAPDH (n = 3/group). (H) WT B6 mice were injected daily intraperitoneally with vehicle, tPA, the tyrosine kinase inhibitor Gleevec, and/or FGFR inhibitor. BMNCs were harvested from mice at day 2 and stained for CD45, Ter119, Sca-1, and PDGFRα and analyzed by flow cytometry. Percentage of PαS-MSCs is given (n = 4/group). (I) Absolute numbers of MSCs in the femur of PBS-, tPA-, EGFR inhibitor–, and PDGFR inhibitor–treated mice was determined by FACS analysis (n = 4/group). Mean ± SEM. $^{*}P < .05$; $^{**}P < .01$; $^{***}P < .001$ by Student *t* test or ANOVA with Tukey HSD tests for multigroup analysis. Data are representative of 2 independent experiments.

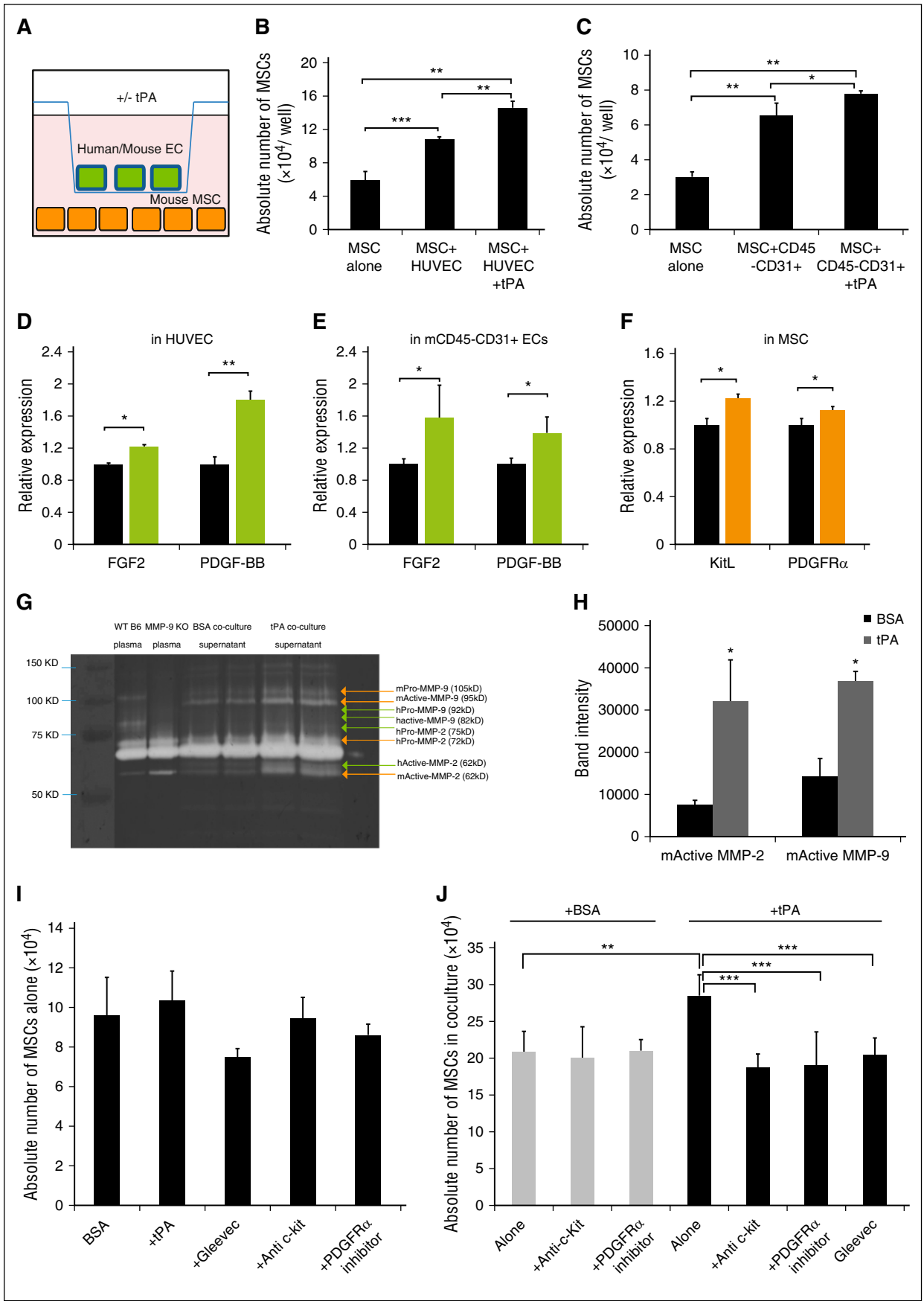

Figure 6.

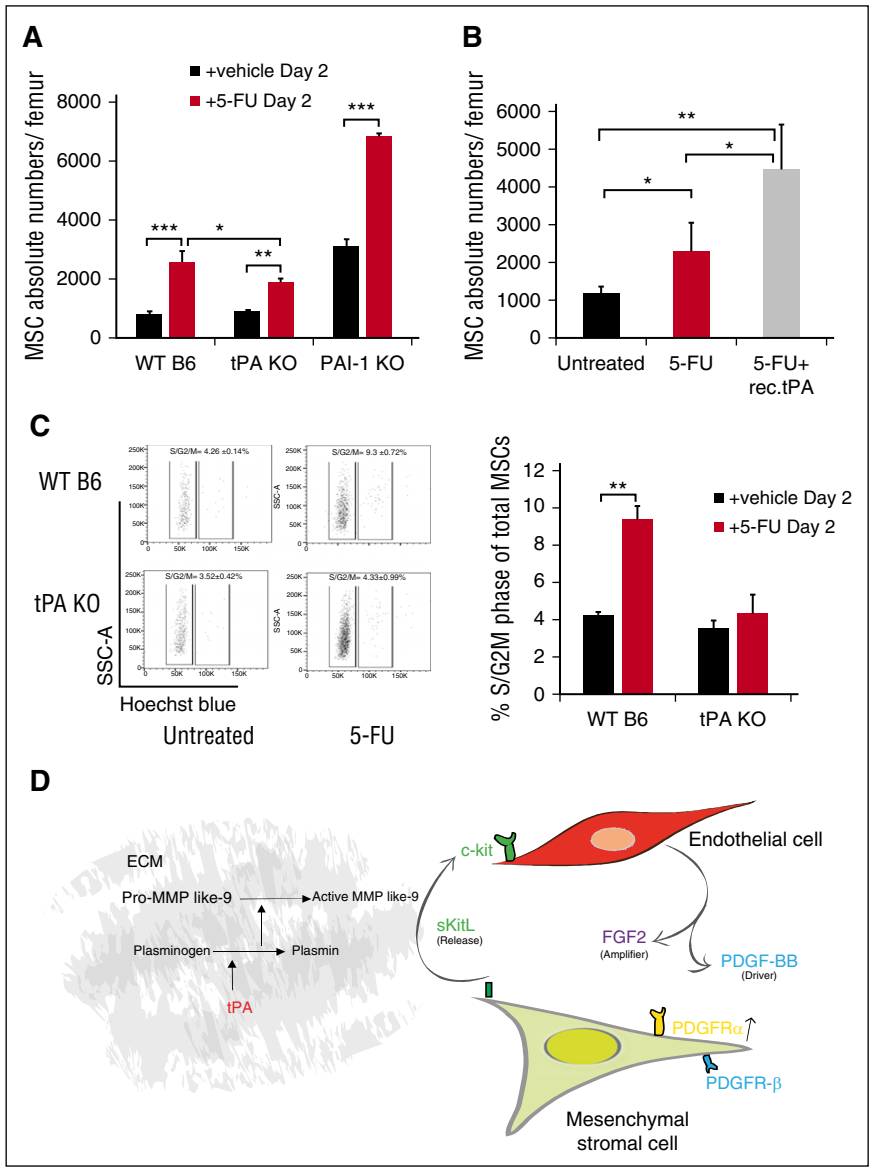

Figure 7. Endogenous tPA is required for PαS-MSC expansion following 5-FU–induced myelosuppression. (A) The absolute numbers of PαS-MSCs per femur from WT B6, *tPA*$^{-/-}$, and *PAI-1*$^{-/-}$ mice 2 days after injection of a single dose of 5-FU was determined by FACS analysis (n = 5/group). (B) The absolute numbers of PαS-MSCs per femur from *tPA*$^{-/-}$ mice treated with vehicle or 5-FU with or without tPA was determined by FACS analysis (n = 4/group). (C) Cell cycle analysis of PαS-MSCs isolated from WT B6 and *tPA*$^{-/-}$ mice treated with vehicle or 5-FU was determined by FACS analysis (n = 4/group) with (left) 1 representative FACS plot and (right) the percentage of PαS-MSCs in S/G2M phase. Mean ± SEM. **P* < .05; ***P* < .01; ****P* < .001 by Student *t* test or ANOVA with Tukey HSD tests for multigroup analysis. Data are representative of 2 independent experiments. (D) Proposed model describing tPA as a key regulator of a crosstalk between ECs and PαS-MSCs. By activating various proteases (eg, plasmin and MMPs), tPA creates a proteolytic niche that enhances the release of KitL from PαS-MSCs. In turn, KitL promotes the release of PDGF-BB and FGF2 from c-Kit^{+} ECs. In synergy FGF2 and PDGF-BB augment PDGFRα expression on PαS-MSCs. Therefore, tPA expands PαS-MSCs within the BM niche by amplifying PDGFR signaling in PαS-MSCs.

is critical for tPA-mediated PαS-MSC expansion. Although immunoreactive KitL was found on PDGFRα^{+} perivascular PαS-MSCs, other cells within the BM can also express immunoreactive KitL. Further studies will be required to identify other tPA-responsive, KitL-secreting cells in the nonhematopoietic environment.[40,41]

FGF2 is a potent mitogen for several mesenchymal cell types.[42] Our data are in agreement with a report demonstrating that increased PA activity enhances FGF2 signaling.[33] FGF2 can also upregulate KitL in Nestin^{+} MSCs.[29] In vitro studies have shown that FGF2, in cooperation with other nonidentified factors and by inducing the expression of PDGFRα and FGFR1/2, promotes proliferation of MSCs without altering their multipotency or inducing their differentiation.[43] In this study, we identified PDGF-BB as a partner that cooperates with FGF2. Gene expression differences within the mesenchymal lineage observed for tPA-treated and control PαS-MSCs are most likely due to differences in how quickly cells progress through the different stages of lineage differentiation, as found for various chondrocytic differentiation genes.[44] Further studies are needed to clarify the fluctuation in

Figure 6. PDGFRα and c-Kit blockade prevents tPA-induced PαS-MSC expansion in EC and PαS-MSCs cocultures. (A) Experimental setting: mouse PαS-MSCs and ECs (mouse CD45^{-}CD31^{+} or human HUVECs) were cocultured with or without recombinant tPA for 3 days and separated from each other using a transwell chamber system. (B-C) The absolute numbers of PαS-MSCs per well after the addition of recombinant tPA or vehicle in cocultures with (B) HUVECs or (C) mouse ECs as determined by hemocytometer counting (n = 3/group). (D) HUVECs or (E) mouse CD45^{-}CD31^{+} ECs were cocultured with or without recombinant tPA: relative mRNA expression of (D) human and (E) mouse FGF2 and PDGF-BB (n = 3/group). Data are normalized to GAPDH. (F) Relative mRNA expression of mouse KitL and mouse PDGFRα derived from mouse PαS-MSCs in MSC-HUVEC cocultures (n = 3/group). Data are normalized to GAPDH. (G) Original gel and (H) densitometric quantification of active mouse MMP-2 and MMP-9 after gelatin zymography in PαS-MSCs from MSC-HUVEC cocultures (n = 3). B6 mouse plasma was used as positive and MMP-9 KO plasma as negative control. (I) Absolute numbers of PαS-MSCs per well in single cultures treated with vehicle, tPA, ACK2, PDGFRα inhibitor, or Gleevec as determined by hemocytometer counting (n = 3/group). (J) The absolute numbers of MSCs per well in MSC-HUVEC coculture with vehicle (white) or tPA (black) with or without ACK2, PDGFRα inhibitor, or Gleevec as determined by hemocytometer counting (n = 4/group). Mean ± SEM. **P* < .05; ***P* < .01; ****P* < .001 by Student *t* test or ANOVA with Tukey HSD tests for multigroup analysis. Data are representative of 3 independent experiments.

expression of differentiation-related genes found in tPA-treated and control PαS-MSCs.

Collectively, these data introduce a novel regulatory mechanism in MSC biology where the fibrinolytic enzyme tPA regulates the MSC and EC content of the BM niche by catalyzing a cytokine crosstalk between ECs and MSCs.

Acknowledgments

The authors thank Matsuzaki (Keio University) for training in MSC isolation; Robert Whittier, Lynett Danks, and Nupur Kohli for proofreading the manuscript; and Zhu Chi for help in statistical analysis.

This work was supported by grants from the Japan Society for the Promotion of Science (Kiban C grant 16K09821 [B.H.] and grant 26461415), Grants-in-Aid for Scientific Research from the Ministry of Education, Culture, Sports, Science and Technology (grant 18013021 to B.H.), Grant-in-Aid for Scientific Research on Innovative Areas (grant 22112007) (B.H.), Health and Labour Sciences Research grant 24 008 (K.H.), a Naito grant (B.H.), and by the collaborative research fund program for women researchers from the Tokyo Medical and Dental University, funded by the "Initiative for Realizing Diversity in the Research Environment," from the Ministry of Education, Culture, Sports, Science and Technology, Japan, in 2016.

Authorship

Contribution: D.D., M.O.-K., and K.S.-K. designed and performed experiments; C.N., and Y.T. gave technical support; S.M., Y.S., S.E., and H.S. discussed and interpreted data; H.N. gave critical advice; and D.D., B.H., and K.H. analyzed data and wrote the paper;

Conflict-of-interest disclosure: The authors declare no competing financial interests.

Correspondence: Beate Heissig, Center for Stem Cell Biology and Regenerative Medicine, Division of Stem Cell Dynamics, The Institute of Medical Science, The University of Tokyo, 4-6-1, Shirokanedai, Minato-ku, Tokyo 108-8639, Japan; e-mail: heissig@ims.u-tokyo.ac.jp.

References

1. Heissig B, Dhahri D, Eiamboonsert S, et al. Role of mesenchymal stem cell-derived fibrinolytic factor in tissue regeneration and cancer progression. *Cell Mol Life Sci.* 2015;72(24):4759-4770.
2. Latsinik NV, Luria EA, Friedenstein AJ, Samoylina NL, Chertkov IL. Colony-forming cells in organ cultures of embryonal liver. *J Cell Physiol.* 1970;75(2):163-165.
3. Friedenstein AJ. Stromal mechanisms of bone marrow: cloning in vitro and retransplantation in vivo. *Haematol Blood Transfus.* 1980;25:19-29.
4. Horwitz EM, Le Blanc K, Dominici M, et al; International Society for Cellular Therapy. Clarification of the nomenclature for MSC: The International Society for Cellular Therapy position statement. *Cytotherapy.* 2005;7(5):393-395.
5. Bianco P, Robey PG, Simmons PJ. Mesenchymal stem cells: revisiting history, concepts, and assays. *Cell Stem Cell.* 2008;2(4):313-319.
6. Zuk PA, Zhu M, Mizuno H, et al. Multilineage cells from human adipose tissue: implications for cell-based therapies. *Tissue Eng.* 2001;7(2):211-228.
7. Young HE, Steele TA, Bray RA, et al. Human reserve pluripotent mesenchymal stem cells are present in the connective tissues of skeletal muscle and dermis derived from fetal, adult, and geriatric donors. *Anat Rec.* 2001;264(1):51-62.
8. Toma JG, Akhavan M, Fernandes KJ, et al. Isolation of multipotent adult stem cells from the dermis of mammalian skin. *Nat Cell Biol.* 2001;3(9):778-784.
9. Fukuchi Y, Nakajima H, Sugiyama D, Hirose I, Kitamura T, Tsuji K. Human placenta-derived cells have mesenchymal stem/progenitor cell potential. *Stem Cells.* 2004;22(5):649-658.
10. Pittenger MF, Mackay AM, Beck SC, et al. Multilineage potential of adult human mesenchymal stem cells. *Science.* 1999;284(5411):143-147.
11. Crisan M, Yap S, Casteilla L, et al. A perivascular origin for mesenchymal stem cells in multiple human organs. *Cell Stem Cell.* 2008;3(3):301-313.
12. Sacchetti B, Funari A, Michienzi S, et al. Self-renewing osteoprogenitors in bone marrow sinusoids can organize a hematopoietic microenvironment. *Cell.* 2007;131(2):324-336.
13. Méndez-Ferrer S, Michurina TV, Ferraro F, et al. Mesenchymal and haematopoietic stem cells form a unique bone marrow niche. *Nature.* 2010;466(7308):829-834.
14. Zhou BO, Yue R, Murphy MM, Peyer JG, Morrison SJ. Leptin-receptor-expressing mesenchymal stromal cells represent the main source of bone formed by adult bone marrow. *Cell Stem Cell.* 2014;15(2):154-168.
15. Morikawa S, Mabuchi Y, Kubota Y, et al. Prospective identification, isolation, and systemic transplantation of multipotent mesenchymal stem cells in murine bone marrow. *J Exp Med.* 2009;206(11):2483-2496.
16. Matsuzaki Y, Mabuchi Y, Okano H. Leptin receptor makes its mark on MSCs. *Cell Stem Cell.* 2014;15(2):112-114.
17. Heissig B, Hattori K, Dias S, et al. Recruitment of stem and progenitor cells from the bone marrow niche requires MMP-9 mediated release of kit-ligand. *Cell.* 2002;109(5):625-637.
18. Heissig B, Lund LR, Akiyama H, et al. The plasminogen fibrinolytic pathway is required for hematopoietic regeneration. *Cell Stem Cell.* 2007;1(6):658-670.
19. Cauwe B, Van den Steen PE, Opdenakker G. The biochemical, biological, and pathological kaleidoscope of cell surface substrates processed by matrix metalloproteinases. *Crit Rev Biochem Mol Biol.* 2007;42(3):113-185.
20. Heissig B, Ohki-Koizumi M, Tashiro Y, Gritli I, Sato-Kusubata K, Hattori K. New functions of the fibrinolytic system in bone marrow cell-derived angiogenesis. *Int J Hematol.* 2012;95(2):131-137.
21. Nishida C, Kusubata K, Tashiro Y, et al. MT1-MMP plays a critical role in hematopoiesis by regulating HIF-mediated chemokine/cytokine gene transcription within niche cells. *Blood.* 2012;119(23):5405-5416.
22. Sato A, Nishida C, Sato-Kusubata K, et al. Inhibition of plasmin attenuates murine acute graft-versus-host disease mortality by suppressing the matrix metalloproteinase-9-dependent inflammatory cytokine storm and effector cell trafficking. *Leukemia.* 2015;29(1):145-156.
23. Heissig B, Ohki M, Ishihara M, et al. Contribution of the fibrinolytic pathway to hematopoietic regeneration. *J Cell Physiol.* 2009;221(3):521-525.
24. Wang X, Lee SR, Arai K, et al. Lipoprotein receptor-mediated induction of matrix metalloproteinase by tissue plasminogen activator. *Nat Med.* 2003;9(10):1313-1317.
25. Rifkin DB, Mazzieri R, Munger JS, Noguera I, Sung J. Proteolytic control of growth factor availability. *APMIS.* 1999;107(1):80-85.
26. Fredriksson L, Li H, Fieber C, Li X, Eriksson U. Tissue plasminogen activator is a potent activator of PDGF-CC. *EMBO J.* 2004;23(19):3793-3802.
27. Dean RA, Cox JH, Bellac CL, Doucet A, Starr AE, Overall CM. Macrophage-specific metalloelastase (MMP-12) truncates and inactivates ELR+ CXC chemokines and generates CCL2, -7, -8, and -13 antagonists: potential role of the macrophage in terminating polymorphonuclear leukocyte influx. *Blood.* 2008;112(8):3455-3464.
28. Ng F, Boucher S, Koh S, et al. PDGF, TGF-beta, and FGF signaling is important for differentiation and growth of mesenchymal stem cells (MSCs): transcriptional profiling can identify markers and signaling pathways important in differentiation of MSCs into adipogenic, chondrogenic, and osteogenic lineages. *Blood.* 2008;112(2):295-307.
29. Rodrigues M, Blair H, Stockdale L, Griffith L, Wells A. Surface tethered epidermal growth factor protects proliferating and differentiating multipotential stromal cells from FasL-induced apoptosis. *Stem Cells.* 2013;31(1):104-116.
30. Itkin T, Ludin A, Gradus B, et al. FGF-2 expands murine hematopoietic stem and progenitor cells via proliferation of stromal cells, c-Kit activation, and CXCL12 down-regulation. *Blood.* 2012;120(9):1843-1855.
31. Tokunaga A, Oya T, Ishii Y, et al. PDGF receptor beta is a potent regulator of mesenchymal stromal cell function. *J Bone Miner Res.* 2008;23(9):1519-1528.
32. Tamplin OJ, Durand EM, Carr LA, et al. Hematopoietic stem cell arrival triggers dynamic remodeling of the perivascular niche. *Cell.* 2015;160(1-2):241-252.
33. Tashiro Y, Nishida C, Sato-Kusubata K, et al. Inhibition of PAI-1 induces neutrophil-driven neoangiogenesis and promotes tissue

regeneration via production of angiocrine factors in mice. *Blood.* 2012;119(26):6382-6393.

34. Ohki M, Ohki Y, Ishihara M, et al. Tissue type plasminogen activator regulates myeloid-cell dependent neoangiogenesis during tissue regeneration. *Blood.* 2010;115(21):4302-4312.
35. Herbert JM, Lamarche I, Prabonnaud V, Dol F, Gauthier T. Tissue-type plasminogen activator is a potent mitogen for human aortic smooth muscle cells. *J Biol Chem.* 1994;269(4):3076-3080.
36. Nissen LJ, Cao R, Hedlund EM, et al. Angiogenic factors FGF2 and PDGF-BB synergistically promote murine tumor neovascularization and metastasis. *J Clin Invest.* 2007;117(10): 2766-2777.
37. Ibrahim AA, Yahata T, Onizuka M, et al. Inhibition of plasminogen activator inhibitor type-1 activity enhances rapid and sustainable hematopoietic regeneration. *Stem Cells.* 2014;32(4):946-958.
38. D'Andrea FP, Horsman MR, Kassem M, Overgaard J, Safwat A. Tumourigenicity and radiation resistance of mesenchymal stem cells. *Acta Oncol.* 2012;51(5):669-679.
39. Sugrue T, Lowndes NF, Ceredig R. Mesenchymal stromal cells: radio-resistant members of the bone marrow. *Immunol Cell Biol.* 2013;91(1):5-11.
40. Ding L, Saunders TL, Enikolopov G, Morrison SJ. Endothelial and perivascular cells maintain haematopoietic stem cells. *Nature.* 2012; 481(7382):457-462.
41. Rafii S, Butler JM, Ding B-S. Angiocrine functions of organ-specific endothelial cells. *Nature.* 2016; 529(7586):316-325.
42. Ornitz DM, Marie PJ. FGF signaling pathways in endochondral and intramembranous bone development and human genetic disease. *Genes Dev.* 2002;16(12):1446-1465.
43. Coutu DL, François M, Galipeau J. Inhibition of cellular senescence by developmentally regulated FGF receptors in mesenchymal stem cells. *Blood.* 2011;117(25):6801-6812.
44. Xu J, Wang W, Ludeman M, et al. Chondrogenic differentiation of human mesenchymal stem cells in three-dimensional alginate gels. *Tissue Eng Part A.* 2008;14(5):667-680.

2016 128: 1063-1075
doi:10.1182/blood-2015-10-673103 originally published online June 9, 2016

Fibrinolytic crosstalk with endothelial cells expands murine mesenchymal stromal cells

Douaa Dhahri, Kaori Sato-Kusubata, Makiko Ohki-Koizumi, Chiemi Nishida, Yoshihiko Tashiro, Shinya Munakata, Hiroshi Shimazu, Yousef Salama, Salita Eiamboonsert, Hiromitsu Nakauchi, Koichi Hattori and Beate Heissig

Blood (print ISSN 0006-4971, online ISSN 1528-0020), is published weekly by the American Society of Hematology, 2021 L St, NW, Suite 900, Washington DC 20036.